Delineation of yield zones using optical and radar remote sensing

Cunha[1], I. A.; Oldoni[2], H.; Melo[1], D.D.; Amaral[1], L.R.

[1] University of Campinas, School of Agricultural Engineering (FEAGRI/UNICAMP), Campinas – SP, Brazil

[2] University of Campinas, Interdisciplinary Center of Energy Planning (NIPE/UNICAMP), Campinas – SP, Brazil

A paper from the Proceedings of the
16th International Conference on Precision Agriculture
21-24 July 2024
Manhattan, Kansas, United States

Abstract.
Identifying yield zones in agricultural areas is essential for efficient resource allocation, operational optimization, and decision-making. While optical remote sensing is widely used in precision agriculture, the interest in radar remote sensing data, notably from the Sentinel-1 Synthetic Aperture Radar (SAR), has increased due to its operation in the C-band frequency, capturing data through cloud cover and the availability of free data. The main objective of this study was to evaluate whether incorporating radar remote sensing data could improve the accuracy of delimiting yield zones compared to relying solely on optical data, as well as to explore the exclusive use of SAR data. Four optical vegetation indices and six different types of SAR data from three soybean and two sorghum crops were acquired during the peak vegetative period. The delimitation of yield zones was carried out through spatial principal component (MULTISPATI-PCA) followed by Fuzzy C-means cluster analysis, complemented by the application of Fuzzy Performance Index (FPI) and Modified Partition Entropy (MPE) functions to determine the optimal number of clusters. These maps were created using only optical data, exclusively SAR data, and a combination of both. Additionally, the soybean and sorghum data were analyzed together and separately. For validation, management zones were created based on actual yield data. The agreement between the resulting maps was evaluated using kappa and z-score indices. The most promising results were obtained when delimiting zones using both optical and SAR data for the grain crops together. In contrast, relying exclusively on SAR data resulted in the worst outcomes. Therefore, the fusion of SAR and optical data enhances the accuracy of delimiting yield zones compared to relying solely on a single data source, highlighting the potential of integrating SAR data in precision agriculture. However, the improvement was not substantial, and the computational cost of generating these images should be considered.

Keywords.
Management zones; Vegetation Index; Synthetic Aperture Radar (SAR).

Introdução

Precision Agriculture (PA) employs techniques and technologies to optimize costs and input usage, addressing the variability of the area. Through PA, it is possible to obtain spatial information about the crop by improving management and decision-making in farm operations (Gebbers and Adamchuk, 2010). Among the techniques used to manage area variability, dividing into management zones subdivides the area and allows for inferences about its homogeneity (Córdoba et al., 2016; Oldoni et al., 2019). These zones are created using input layers of georeferenced data, such as soil and plant data. Utilizing information on plant variability is crucial in delineating management zones. Yield maps correspond more accurately to plant information, but there are several challenges in obtaining this information, from availability to data reliability. Thus, plant information derived from remote sensing is a viable alternative for use in management zones (Almeida et al., 2023).

In PA, remote sensing has been widely used due to the availability of historical data, such as the Landsat and Sentinel-2 series. This allows for obtaining various information about crops through spectral bands and vegetation indices (Castaldi, 2021). However, data collection through these sensors is limited due to cloud interference and the inability to image during nighttime (Silveira et al., 2017). Alternatively, radar remote sensing has been studied for agricultural purposes, including monitoring, mapping, and crop classification (Nasirzadehdizaji et al., 2021; Mestre-Quereda, 2020). The Synthetic Aperture Radar (SAR) sensor operates in the microwave wavelength range, experiencing little atmospheric attenuation, thus allowing data collection from agricultural areas even in cloudy weather or at night. Additionally, depending on the wavelength, it is possible to obtain information about the soil and the canopy (Moran et al., 1998).

The Sentinel-1 mission is equipped with an onboard SAR sensor, operating in the C-band of microwaves (5.54 cm) (ESA, 2024). Although the C-band has limitations in canopy penetration, it provides different information from optical sensors (Bahrami et al., 2021). While optical sensors reveal aspects of the top of the vegetation cover, SAR sensors capture part of the energy reflected by leaves and branches in the canopy depending on the density, allowing inferences about geometry and water content (ULABY et al., 1984). These data enable the extraction of backscatter coefficients (sigma) and the performance of polarimetric decomposition, resulting in entropy and alpha angle. The backscatter response is sensitive to vegetation dynamics, increasing as the plant fills with leaves and increases in volume (LI et al., 2023). This greater interaction with the leaves significantly impacts backscatter results during the crop's development stage (Wali et al., 2020). Additionally, backscatter coefficients are highly sensitive to the presence of water (Nasirzadehdizaji et al., 2021). Polarimetric decomposition allows for crop monitoring and the identification of some crops due to its sensitivity to the target's physical structure (Harfenmeister et al., 2021; Wang et al., 2016; Cloude and Pottier, 1997). Furthermore, like in optical remote sensing, vegetation indices provide information about crops more efficiently and can be applied similarly to SAR data.

Remote sensing data is an alternative for obtaining area information when other data and resources are unavailable. They allow for the collection of spectral behavior information of the area, transforming it into spatial information and managing it more efficiently than without any prior knowledge. The adoption of management zones is an important activity to address spatial variability (Oldoni et al., 2019). However, there is a gap in knowledge regarding the incorporation of SAR data for their delineation. In this sense, the objective of this study was to evaluate whether the use of radar remote sensing data can delineate yield zones or enhance the accuracy of delineating yield zones compared to relying solely on optical data, providing an additional resource for specialized crop management.

Material and Methods

This study analyzes SAR images for the creation of yield zones in soybean and sorghum crops.

The study was conducted in a commercial production area of approximately 106 hectares, located in the municipality of Cosmópolis, SP, Brazil (22°41'55.16"S and 47°10'34.15"W). Figure 1 presents the diagram of the study design.

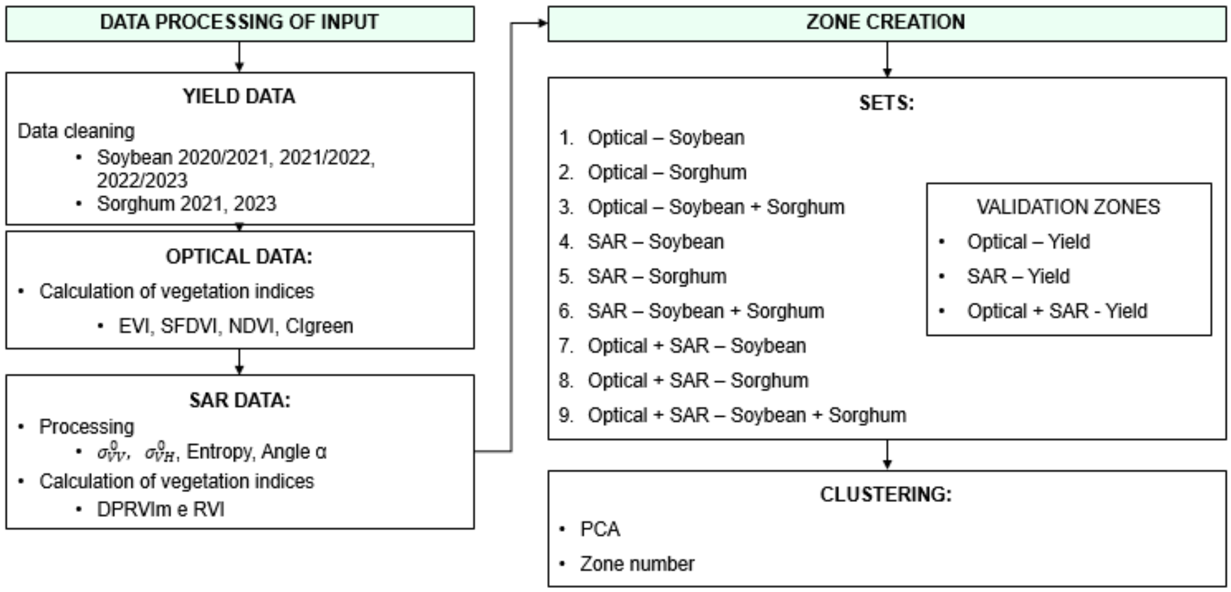

Fig. 1 – Delineamento do trabalho realizado.

Grain yield data from three soybean harvests (2020/2021, 2021/2022, and 2022/2023) and two intercropping seasons of sorghum (2021 and 2023) were obtained through a yield monitor installed on the combine harvester. To ensure data quality, outliers and inliers resulting from different factors, such as incorrect adjustment of the platform width, maneuvers performed by the harvester, and sensor failures (Menegatti and Molin, 2004), were removed using the procedure suggested by Maldaner et al. (2021). Next, ordinary kriging was used for data interpolation (Figure 2), with the best fit of the experimental semivariogram by the spherical model.

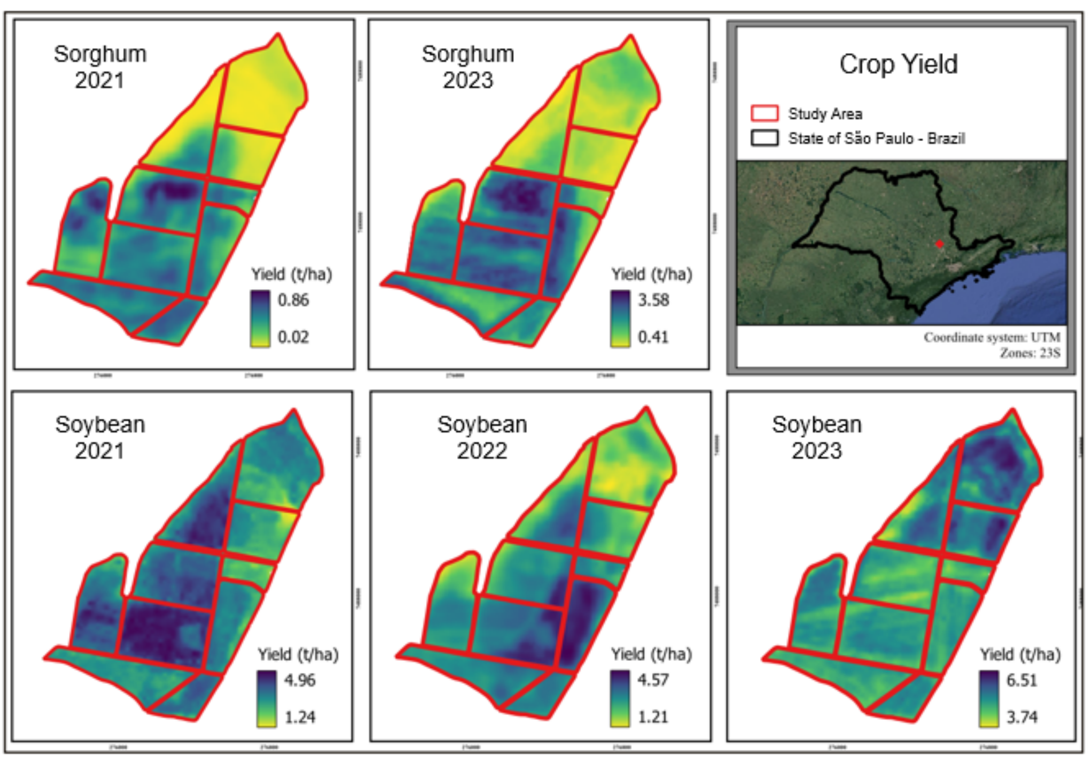

Fig. 2 – Interpolated yield maps of the five crop seasons

For the optical data, Sentinel-2 images were acquired with Level 2A atmospheric correction during the peak vegetative stage, and Sentinel-1 SAR sensor data on dates close to those of the optical data (Table 1). The peak vegetative stage was determined using a time series based on the Enhanced Vegetation Index (EVI). From the optical images, it was calculated four vegetation indices (Table 2) to obtain different information on crop reflectance.

Table 1. Dates corresponding to the acquisition of optical and SAR data for the crops.

Crop	Harvest	Data S1	Data S2
Soybean	2020/2021	03/02/2021	03/02/2021
Sorghum	2021	27/06/2021	20/06/2021
Soybean	2021/2022	10/02/2022	15/02/2022
Soybean	2022/2023	05/02/2023	08/02/2023
Sorghum	2023	17/06/2023	18/06/2023

The SAR sensor operates in the C-band, and the European Space Agency (ESA) provides the data free of charge. We acquired SAR data at Level 1 SLC (Single Look Complex) in the IW (Interferometric Wide) mode, where the sensor operates in dual polarization: VH (vertical transmission and horizontal reception polarization) and VV (vertical transmission and reception polarization). This acquisition configuration allows for obtaining both backscatter coefficient data and polarimetric decomposition for dual polarizations (Cloude, 2007).

Table 2. Índices de Vegetação ópticos calculados.

	Vegetation Index	Equation
EVI	Enhanced vegetation index	2.5(NIR − Red) / (NIR + 6Red − 7.5Blue + 1)
SFDVI	Spectral Feature Depth Vegetation Index	[(NIR+Green)/2] –[(R+REDEDGE1)/2]
NDVI	Normalized difference vegetation index	(NIR+Red)(NIR−Red)
CI	Chlorophyll index (with green band)	(NIR / Green) – 1

It was conducted that SAR image processing, as recommended by Diniz (2019) to extract backscatter coefficients (σ_VV^0, σ_VH^0) (Figure 3a), as well as polarimetric decomposition that generated corresponding images of the alpha angle and entropy (Figure 3b). Based on the backscatter coefficients, it was calculated the Radar Forest Degradation Index (RFDI), which aids in differentiating vegetation types and providing more information from dual-polarization data (MITCHARD et al., 2012). Through polarimetric decomposition processing, it was obtained that the Dual-Pol Radar Vegetation Index (DPRVI), proposed by Mandal et al. (2020), which utilizes Cloude and Pottier's (1996) polarimetric decomposition to calculate the normalized dominant eigenvalue and degree of polarization, allowing for crop monitoring. After generating the SAR images (σ_VV^0, σ_VH^0, H, alpha angle, RFDI, and DPRVI), it was clipped these images with a distance of 15 meters from the pathways to avoid external influences on the crop. Additionally, these indices were standardized on a scale from 0 to 1 to facilitate comparison between variables.

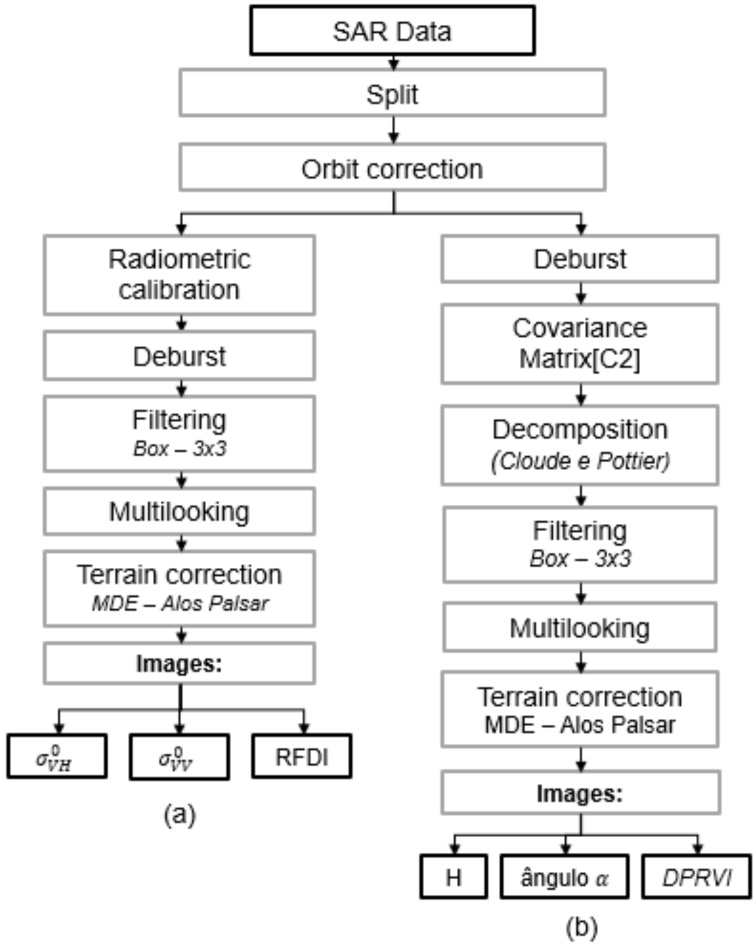

Fig. 3 - Processing flow of SAR images for backscatter coefficient data (a) and for polarimetric decomposition (b).

The delineation of productivity zones was carried out using spatial principal component analysis (MULTISPATI-PCA), followed by Fuzzy C-means cluster analysis, as per Córdoba et al. (2016). This approach reduces data collinearity, allowing for determining the most suitable number of zones for each dataset. The definition of the number of principal components (PCs) used in clustering depends on the explained cumulative variance, where a minimum value of 70% was adopted. Two cluster quality indices were applied to determine the ideal number of clusters (zones): Fuzzy Performance Index (FPI) and Modified Partition Entropy (MPE), where lower values indicate a more suitable number of zones.

Different numbers of zones were explored, ranging from 2 to 5, in nine distinct scenarios. This included the analysis of both crops separately (soybean and sorghum), as well as combined (soybean+sorghum), and the use of SAR and optical data individually and combined (SAR, optical, and SAR+optical). Three reference scenarios were also considered based on soybean, sorghum, and soybean+sorghum yield data.

Results e discussion

During the implementation of spatial PCA for the tested scenarios, the number of principal components explaining more than 70% of the cumulative variance ranged from 2 to 4 (Table 3). Using only a remote sensing approach (optical or SAR) for sorghum, only two principal components (PCs) were needed, while soybean required three PCs to reach 70%. This difference can be attributed to the amount of input data: sorghum had data from only two harvests, while soybean had data from three harvests. This indicates a certain discrepancy in yield behavior over the years. Additionally, when using combined optical and SAR data, the number of necessary PCs increased to 3 and 4, respectively, indicating that a higher amount of input data influences the process of defining PCs. The indices that stood out the most in the first PCs were SFDVI for soybean and NDVI and SFDVI for sorghum (Figure 4). When integrating both crops, in addition to these indices, CIgreen also stood out. The last component in all cases highlighted the DPRVI index, indicating that SAR data, especially those formed by the polarimetric decomposition process, influence principal component analysis and consequently provide additional information to optical VIs.

Table 3. Explained variance (V) and the total explained variance (V_{acu}), in %, of the spatial principal components (PCs) applied to the different scenarios and the number of PCs adopted to reach at least 70% (N).

PC	Optical						SAR						SAR + Optical					
	Soybean		Sorghum		Soybean + sorghum		Soybean		Sorghum		Soybean + sorghum		Soybean		Sorgo		Soybean +Sorghum	
	V	V_{acu}	V	V_{acu}	V	V_{acu}	V	V_{acu}	V	V_{acu}	V	V_{acu}	V	V_{acu}	V	V_{acu}	V	V_{acu}
1	42	42	63	63	53	53	30	30	37	37	27	27	32	32	47	47	40	40
2	26	69	20	84	16	70	27	57	34	71	20	48	15	47	18	66	14	54
3	12	81					22	79			14	63	13	60	13	88	9	64
4											11	74	9	70			5	70
N	3		2		2		3		2		4		4		3		4	

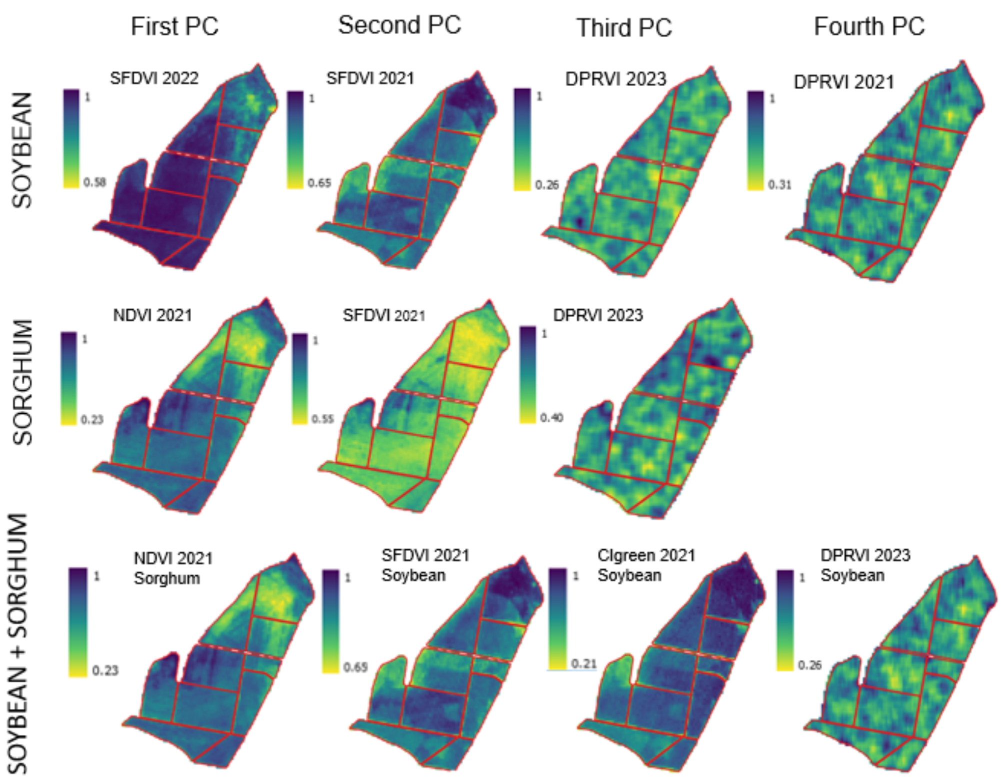

Fig. 4 – Variables that stood out in the principal component analysis explaining more than 70% of the cumulative variance in scenarios integrating SAR and optical data.

Based on FPI and MPE indices, three zones would be indicated for soybean, two for sorghum, and also two zones when both crops were analyzed together (Figure 5). Additionally, the option for 2 zones is not viable when exclusively using SAR data due to the higher values obtained. SAR data produce images with different patterns than optical images (Figure 4), as they provide information affected by distinct variables such as volume, geometry, and surface moisture (LI et al., 2023; Harfenmeister et al., 2021; Nasirzadehdizaji et al., 2021), which are not related to vegetative vigor as with optical indices. Furthermore, when including SAR data with optical data, the indices tended to follow the same pattern as optical data and resembled productivity data more closely. Therefore, it was decided to proceed with the study using two zones.

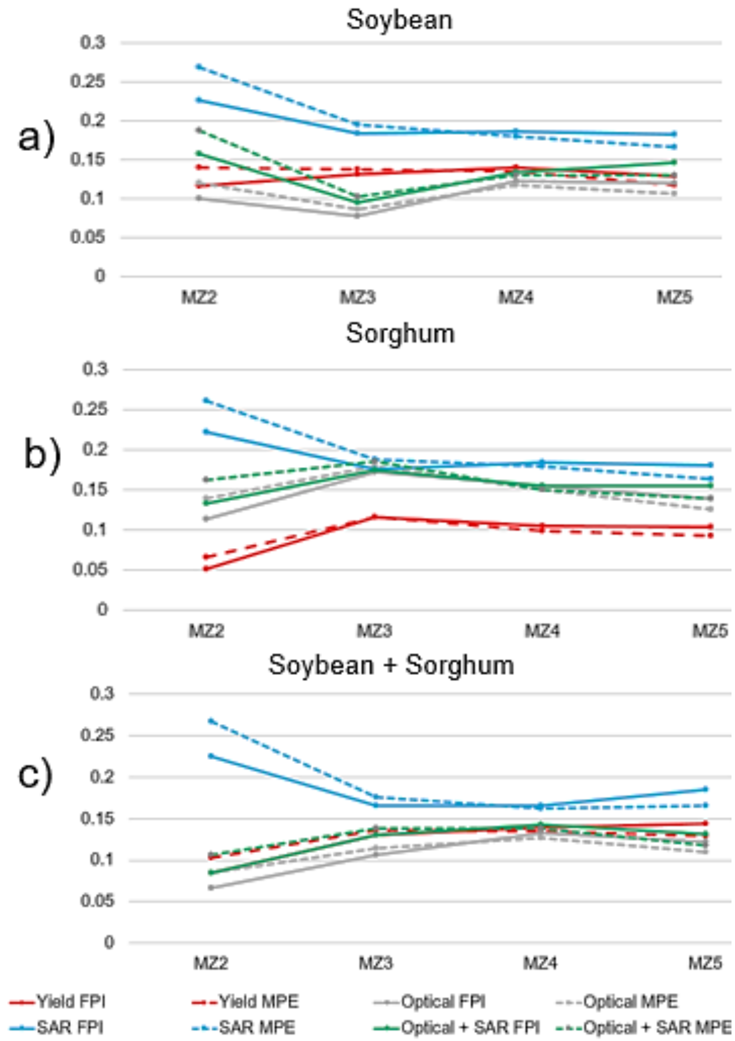

Fig. 5 – Cluster quality indices (MPE and FPI) for scenarios with soybean (a), sorghum (b), and using soybean and sorghum together (c).

Upon analyzing the similarity between actual productivity maps and those obtained through remote sensing using the kappa coefficient, it was found that the integrated use of SAR and optical data yields better results than using each type of data alone (Table 4). Despite radar wave penetration in the C-band depending on canopy density (Bahrami et al., 2021), and the higher canopy density at the vegetative peak, SAR data still added information to optical data. Although SAR data showed the greatest discrepancy compared to productivity data, they were significant in augmenting clustering with optical data, as indicated by the Z score. However, despite SAR data improving productivity zone definition, the improvement when including them was less than 10%, considering the kappa index. The high computational cost of generating this data is a disadvantageous point. Therefore, the decision to include SAR data should consider the balance between marginal accuracy benefits and associated computational costs.

Table 4. Kappa index, z score, and the percentage difference in kappa when using SAR data along with optical data using two zones.

	Soybean		Sorghum		Soybean + Sorghum	
	Kappa	z-score	Kappa	z-score	Kappa	z-score
Optical	0.527	85.5	0.633	103	0.663	32.6

SAR	0.077	12.5	0.276	44.8	0.226	11.1
Optical + SAR	0.573	93.1	0.645	105	0.704	34.7
Difference	8%		2%		6%	

The integrated use of SAR and optical data yielded better results in terms of productivity zone delineation, especially when integrating both crops. In addition to this statistical finding through kappa and z score (Table 4), the similarity between productivity zones created by actual productivity data and those derived from remote sensing images can also be visually observed (Figure 6). This suggests that data diversity provides information from more than one crop and can delineate better productivity zones, even with different phenologies, resulting in better similarity with actual productivity. Therefore, integrating remote sensing data from different sources and crops can improve accuracy in delineating management zones.

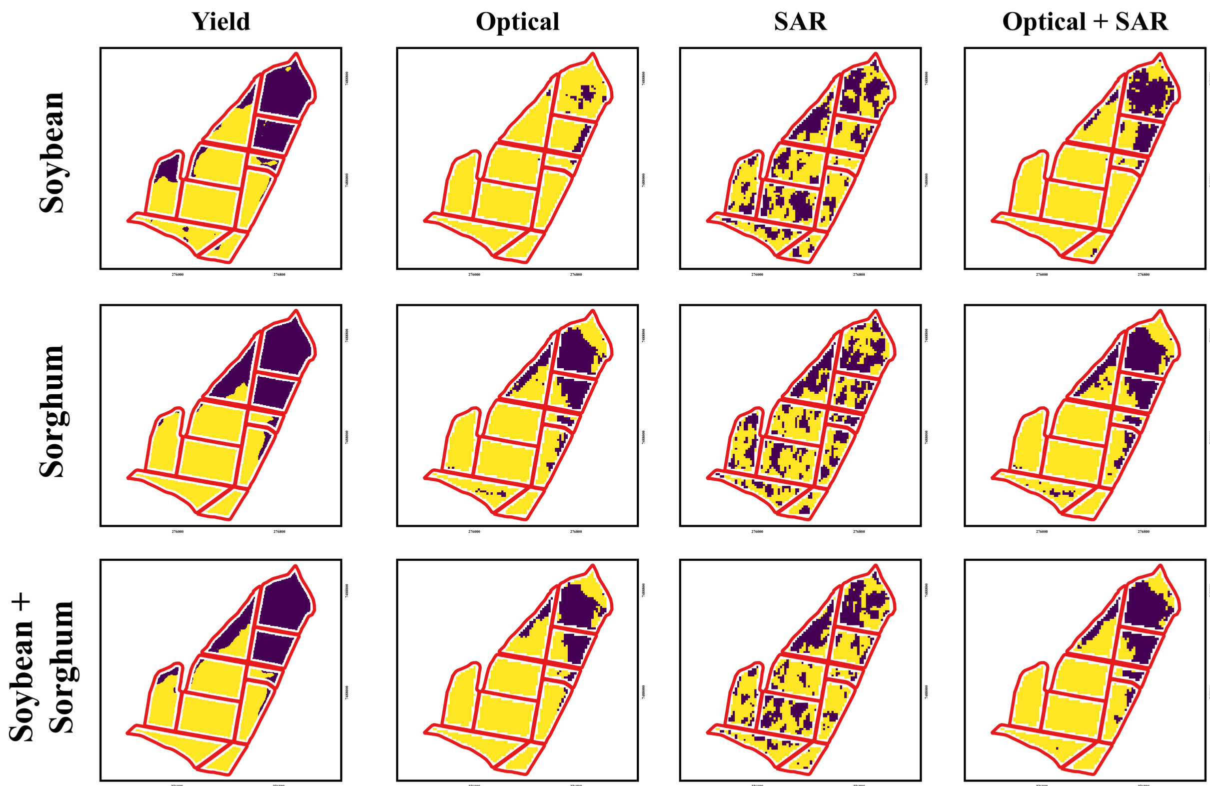

Fig. 6 – Productivity zone maps (2 zones) for soybean and sorghum crops individually and combined, created using productivity data (reference), only optical remote sensing information (optical), SAR sensing, and integrating both pieces of information (Optical+SAR).

Conclusion

Compared to sole reliance on optical data, the incorporation of SAR data in defining productivity zones may increase similarity with zones determined by the productivity map. However, it is crucial to consider the high operational cost associated with obtaining SAR data, which may render this approach unfeasible in some situations.

Acknowledgments

This research was supported by the Coordenação de Aperfeiçoamento de Pessoal de Nível Superior - Brazil (CAPES) - Financing Code 001 and by the Fundação de Amparo à Pesquisa do Estado de São Paulo - FAPESP (process number 2022/03160-8). We would like to thank São José Farm for providing the study area and productivity data.

References

Castaldi, Fabio. (2021). Sentinel-2 and Landsat-8 multi-temporal series to estimate topsoil properties on croplands. Remote Sensing, 13(17), 3345.

Cloude, S. R. (2007). The dual polarization entropy/alpha decomposition: a PALSAR case study. In POLINSAR WORKSHOP, Frascati, Italy. Abstracts… Frascati: ESA, p.19.

Cloude, Shane R., & POTTIER, Eric. (1997). An entropy based classification scheme for land applications of polarimetric SAR. IEEE Transactions on Geoscience and Remote Sensing, 35(1), 68-78.

Córdoba, M. A., BRUNO, C. I., COSTA, J. L., PERALTA, N. R., & BALZARINI, M. G. (2016). Protocol for multivariate homogeneous zone delineation in precision agriculture. Biosystems Engineering, 143, 95-107.

Diniz, J. M. F. S. (2019). Evaluation of the potential of Sentinel-1A polarimetric data for land use and land cover mapping in the Ariquemes region - RO. Master's Dissertation in Remote Sensing, National Institute for Space Research, São José dos Campos. xxvi + 134 p. Advisor: Dr. Fábio Furlan Gama.

European Space Agency (ESA). (2023). Sentinel-1 SAR technical guide. Available at: https://sentinels.copernicus.eu/web/sentinel/technical-guides/sentinel-1-sar. Accessed: January 18, 2023.

Figueiredo, Divino. (2005). Basic concepts of remote sensing. São Paulo.

Fountas, S., Espejo-García, B., Kasimati, A., Mylonas, N., & Darra, N. (2020). The future of digital agriculture: technologies and opportunities. IT Professional, 22(1), 24-28.

Harfenmeister, K., Itzerott, S., Weltzien, C., & Spengler, D. (2021). Agricultural monitoring using polarimetric decomposition parameters of Sentinel-1 data. Remote Sensing, 13(4), 575.

Jensen, John R. (2009). Remote sensing of the environment: An earth resource perspective 2/e. Pearson Education India.

Li, Zhenwang, et al. (2023). Synergetic use of DEM derivatives, Sentinel-1 and Sentinel-2 data for mapping soil properties of a sloped cropland based on a two-step ensemble learning method. Science of The Total Environment, 161421.

Maldaner, L.F., Canata, T.F., & Molin, J.P. (2022). An approach to sugarcane yield estimation using sensors in the harvester and Zigbee technology. Sugar Tech, 24, 813-821.

MandaL, Dipankar, et al. (2020). Dual polarimetric radar vegetation index for crop growth monitoring using Sentinel-1 SAR data. Remote Sensing of Environment, 247, 111954.

Menegatti, Leonardo A.A., & MOLIN, José P. (2004). Removal of errors in yield maps via raw data filtering. Revista Brasileira de Engenharia Agrícola e Ambiental, 8, 126-134.

Mestre-Quereda, A., Lopez-Sanchez, J. M., Vicente-Guijalba, F., Jacob, A. W., & Engdahl, M. E. (2020). Time-series of Sentinel-1 interferometric coherence and backscatter for crop-type mapping. IEEE Journal of Selected Topics in Applied Earth Observations and Remote Sensing, 13, 4070-4084.

Mitchard, E. T. A., et al. (2012). Mapping tropical forest biomass with radar and spaceborne LiDAR in Lopé National Park, Gabon: Overcoming problems of high biomass and persistent cloud. Biogeosciences, 9(1), 179–191.

Molin, José Paulo, DO AMARAL, Lucas Rios, & COLAÇO, André. (2015). Precision agriculture. Oficina de textos.

Moran, M. Susan, et al. (1998). Ku-and C-band SAR for discriminating agricultural crop and soil conditions. IEEE Transactions on Geoscience and Remote Sensing, 36(1), 265-272.

Nasirzadehdizaji, Rouhollah, et al. (2019). Sensitivity analysis of multi-temporal Sentinel-1 SAR parameters to crop height and canopy coverage. Applied Sciences, 9(4), 655.

Nasirzadehdizaji, Rouhollah, et al. (2021). Sentinel-1 interferometric coherence and backscattering analysis for crop monitoring. Computers and Electronics in Agriculture, 185, 106118.

Ohana-Levi, N., Knipper, K., Kustas, W. P., Anderson, M. C., Netzer, Y., Gao, F., ... & Karnieli, A. (2020). Using satellite thermal-based evapotranspiration time series for defining management zones and spatial association to local attributes in a vineyard. Remote Sensing, 12(15), 2436.

Oldoni, Lucas Volochen, et al. (2019). Characterization of the dynamics of soybean, corn, and cotton based on polarimetric SAR data from Sentinel-1a. In Anais XIX Simpósio Brasileiro de Sensoriamento Remoto, 692-695.

Oldoni, H., Terra, V. S. S., Timm, L. C., Júnior, C. R., & Monteiro, A. B. (2019). Delineation of management zones in a peach orchard using multivariate and geostatistical analyses. Soil and Tillage Research, 191, 1-10.

Prudente, Victor Hugo Rohden, et al. (2019). Relationship between SAR/Sentinel-1 polarimetric and interferometric data with biophysical parameters of agricultural crops. International Archives of the Photogrammetry, Remote Sensing & Spatial Information Sciences.

Richetti, J., Judge, J., Boote, K. J., Johann, J. A., Uribe-Opazo, M. A., Becker, W. R., ... & Silva, L. C. D. A. (2018). Using phenology-based enhanced vegetation index and machine learning for soybean yield estimation in Paraná State, Brazil. Journal of Applied Remote Sensing, 12(2), 026029-026029.

Rouze, G., Neely, H., Morgan, C., et al. (2021). Evaluation of images from unmanned aerial systems (UAS) as an alternative tool for cotton-based management zones. Precision Agriculture, 22, 1861–1889. https://doi.org/10.1007/s11119-021-09816-9

Schlund, Michael, & Erasmi, Stefan. (2020). Sentinel-1 time series data for monitoring the phenology of winter wheat. Remote Sensing of Environment, 246, 111814.

Silveira, H. L. F., Eberhardt, I. D. R., Sanches, I. D. A., & Galvão, L. S. (2017). Cloud cover analysis in northeastern Brazil and its impacts on operational agricultural remote sensing.

Ulaby, Fawwaz T., & JEDLICKA, R. P. (1984). Microwave dielectric properties of plant materials. IEEE Transactions on Geoscience and Remote Sensing, (4), 406-415.

Wali, E., Tasumi, M., & Moriyama, M. (2020). Combination of linear regression lines to understand the response of Sentinel-1 dual polarization SAR data with crop phenology—case study in Miyazaki, Japan. Remote Sensing, 12(1), 189.

Wang, Hongquan, Magagi, Ramata, & Goita, Kalifa. (2016). Polarimetric decomposition for monitoring crop growth status. IEEE Geoscience and Remote Sensing Letters, 13(6), 870-874.

You, J., Li, X., Low, M., Lobell, D., & Ermon, S. (2017). Deep Gaussian Process for Crop Yield Prediction Based on Remote Sensing Data. Proceedings of the AAAI Conference on Artificial Intelligence, 31(1).